JACS
JOURNAL OF THE AMERICAN CHEMICAL SOCIETY
Article
pubs.acs.org/JACS

Proton Gradient-Induced Water Transport Mediated by Water Wires Inside Narrow Aquapores of Aquafoldamer Molecules

Huaiqing Zhao,[†,∥,⊥] Shen Sheng,[†,⊥] Yunhan Hong,[‡] and Huaqiang Zeng*[,§]

[†]Department of Chemistry, 3 Science Drive 3, National University of Singapore, Singapore 117543
[‡]Department of Biological Science, 14 Science Drive 4, National University of Singapore, Singapore 117543
[§]Institute of Bioengineering and Nanotechnology, 31 Biopolis Way, The Nanos, Singapore 138669

Supporting Information

ABSTRACT: Hollow tubular aquapores inside aquafoldamers can be created via the "sticky" end-mediated formation of 1D chiral helical stacks involving same-handed helices, and are capable of aligning H-bonded water molecules in a chain-like fashion. These aquapores uniquely feature a small cavity of ∼2.8 Å in diameter, a size identical to that of the water molecule and also comparable to the narrowest opening in naturally occurring aquaporins measuring ∼3 Å across, and hence allow not only proton transport but also unique proton-gradient-induced water transport across the lipid membranes in the presence of proton gradient.

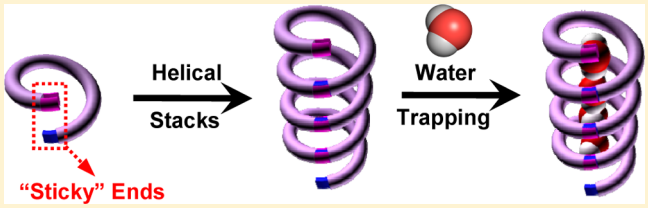

INTRODUCTION

Aquaporins contain one-dimensionally arrayed H-bonded water chains in their narrow channels with the narrowest pore diameter measuring ∼3 Å. This narrow pore constriction synergistically works with the two conserved asparagines in the center of the channel to serve as the selectivity filter to permit the preferential diffusion of water molecules of ∼2.8 Å in diameter over protons and other species across the cell membrane.[1] Their structure and function have thus provided an inspiring target for mimicking by synthetic water channels. In addition to carbon nanotubes[2a,b] and coordination complexes,[2c] a limited number of channel-forming organic molecules have also been reported that contain either hydrophilic[3] or hydrophobic[4] pores, which are capable of accommodating H-bonded 1D water chains and mediating efficient transport of water molecules[3f,5a−c] and protons[3f,5a,d,e] across the bilayer membrane.

Over the past few years, we have been investigating the possibility of using water-binding foldamer molecules, termed aquafoldamers,[6a] to mimic aquaporins with an ultimate aim to realize synthetic water channels for rapid and selective transport of water molecules. The ability to do so may help to elucidate the key structural determinants for achieving transmembrane transport of small chemical species, and may further lead to various important applications including ultrapure water production. Toward this goal, we have designed a series of pyridine-based aquafoldamers as illustrated by oligoamides **1** (Figure 1a).[6] Structurally enforced by intramolecular H-bonding networks, these molecules fold into a crescent structure to enclose a suitable water-binding cavity of ∼2.8 Å in diameter defined by the interior amide protons. Oligomers containing four or more repeating units such as **1a** adopt a helical structure possessing about 4.3 residues per helical turn.[6b] Functionally, trimers with a planar geometry bind one water molecule in their 2D planar cavity, while helically folded longer oligomers such as **1a** are able to accommodate two water molecules in their 3D-shaped helical cavity (Figure 1b).[6a,c]

Although aquafoldamers such as **1a** and other closely related analogues[6a,c] can bind water molecules with good affinities, the packing among the water complexes (Figure 1b) is disfavored toward the creation of 1D hollow tubular cavities for encapsulating 1D water chains. Since a full overlap of helically folded aromatic backbones via aromatic $\pi-\pi$ stacking forces is apparently energetically more favored than the side-by-side overlap involving helical backbones, we have been greatly puzzled by the zigzag packing seen in **1a** (Figure 1b) and a predominant occurrence of partial overlaps seen in many other helical foldamers with known crystal structures.[7a,b] Careful analysis of these helical structures shows that most of them contain end groups that electrostatically repel, rather than attract, each other. Recently, we postulated that, by incorporating two electrostatically complementary functional groups into the two helical ends, the resultant helices possessing "sticky" ends might be able to efficiently pile up via full overlaps to form one-dimensionally aligned helical chiral stacks involving same-handed helices. If the helical molecules contain a cavity, such 1D packing should further create a hollow tubular cavity for inclusion of guest molecules.[7c] Our subsequent testing of this hypothesis using **1b** having two complementary "sticky" ends, i.e., the ester and Cbz ends in Figure 1c, indeed demonstrates the ability of the two "sticky" ends to promote efficient 1D chiral stacking among the helices of the same, rather than opposite, handedness (Figure 1d). The

Received: August 7, 2014
Published: September 16, 2014

dx.doi.org/10.1021/ja5077537 | J. Am. Chem. Soc. 2014, 136, 14270−14276

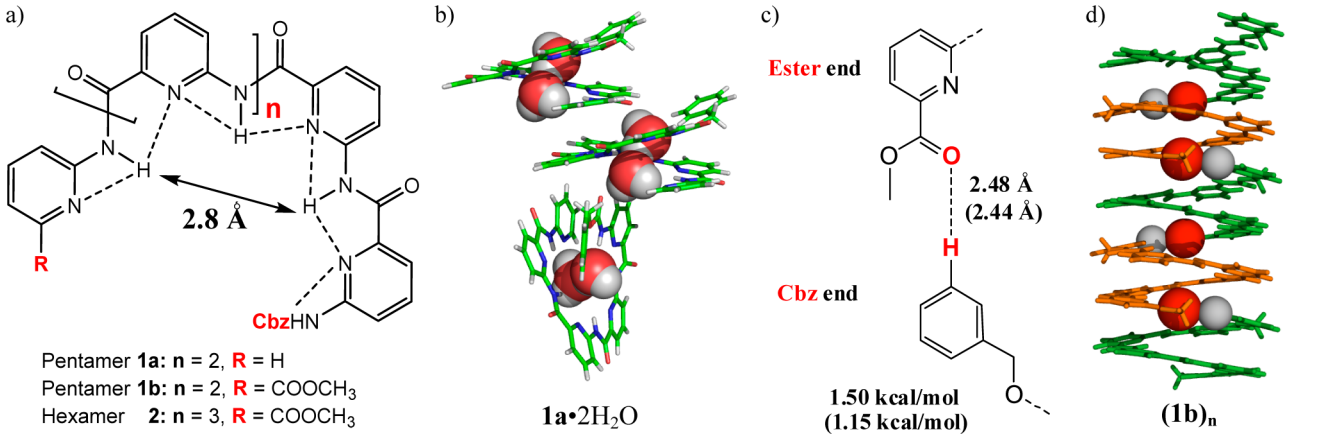

Figure 1. (a) Structures of aquafoldamers **1** and **2** containing an interior cavity of ~2.8 Å in diameter, which is defined by the interior amide protons, (b) intermolecular zigzag packing by water complex **1a**·2H_2O, (c) "sticky" end groups (ester and Cbz) from **1b** that are complementary to each other by virtue of a partially charged O atom (H-bond acceptor) and an aromatic proton (H-bond donor), which are able to form a weak intermolecular H-bond; this H-bond was computationally determined to have a bond length of 2.48 Å and 1.50 kcal/mol at the B3LYP/6-311G(2d,p) level, and crystallographically found to measure 2.44 Å in length with a computationally determined bond strength of 1.15 kcal/mol, and (d) 1D chiral packing of left-handed **1b** via complementary "sticky" end groups shown in (c) and aromatic $\pi-\pi$ stacking forces. In (d), the complementary O and H atoms shown in (c) from the ester and Cbz ends are represented as red and gray balls, respectively.

1D tubular cavity thus created was also found to contain 1D chains of methanol or dichloromethane molecules.[7c]

RESULTS AND DISCUSSION

Interestingly, even after regrowing the crystals of **1b** in water-containing solvents, the structural determinations of the "water-soaked" crystals reveal that only 24–40% of the MeOH molecules inside the interior of $(\mathbf{1b})_n$ were replaced by water molecules. This is in sharp contrast with the fact that other analogous oligomers such as **1a** can fully accommodate two water molecules in their cavity.[6a,c] This suggests that the hollow cavity in $(\mathbf{1b})_n$ is functionally selective and displays higher binding affinities toward methanol or dichloromethane than water molecules. Our observations in some other cases also suggest that water binding by these pyridine analogues exhibit strong dependence on the end groups, oligomeric length or even exterior side chains. Accordingly, while a trimer containing an exterior side chain at its ester end and a tetramer were both found to contain no water molecules in their cavity, other analogous trimers and pentamers do bind water molecules in the solid states.[6a,c]

Therefore, despite the fact that **1b** is unable to host water molecules in its tubular cavity, it is our belief that by some modifications in oligomeric length, repeating unit or end group, it might still be possible to produce the same type of 1D chiral stack with an enclosed tubular aquapore suitable for water recognition and transportation. To validate this hypothesis, we set out to test four oligomeric molecules **2**–**4** (Figures 1a and 2a).

The first oligomer we tested was hexamer **2** with one more repeating unit than pentamer **1b**. With an elongated backbone, the chemical microenvironment in **2** must differ from that in **1b**, possibly allowing for **2** to bind water molecules. On the other hand, **2**, containing two "sticky" end groups identical to those in **1b**, is expected to form 1D helical stacks similar to those formed from **1b**.

As a result of efficient backbone rigidification by a continuous intramolecular H-bonding network made up of 11 H-bonds ranging from 2.127 to 2.408 Å in length, the crystal structure of **2** similarly illustrates a crescent-shaped helical structure (Figure

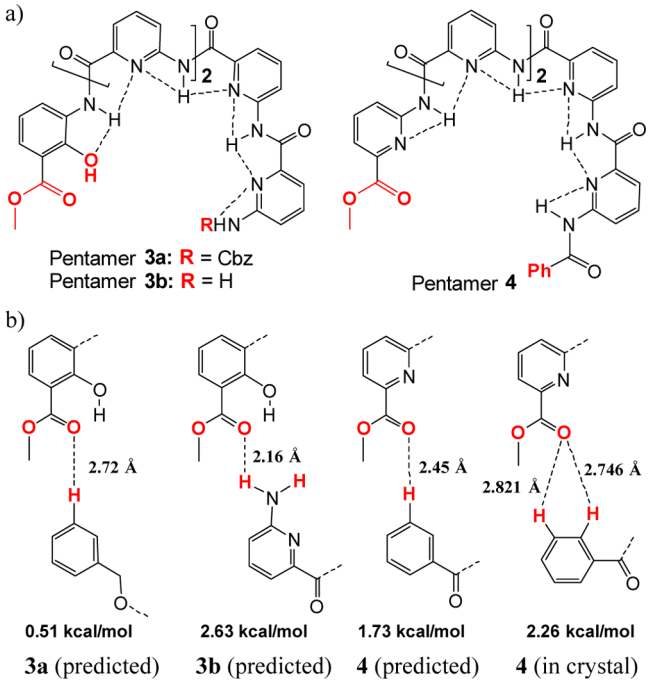

Figure 2. (a) Structures of pentamers **3** and **4** for testing possible formation of 1D helical stacks mediated by the H-bond patterns involving the two "sticky" ends shown in (b). The bond strengths of H-bonds in (b) were calculated at the level of B3LYP/6-311G(2d,p). Further, the predicted H-bond pattern between the two "sticky" ends in **4** slightly differs from that observed in the solid state, and the predicted H-bond patterns for both **3a** and **3b** were not observed experimentally.

3a,b). As expected, the enclosed small cavity of about ~2.8 Å in diameter defined by the interior amide protons is able to host two water molecules per molecule of **2** in a way similar to other analogous pentamers.[6a,c] The water dimer cluster in **2** is stabilized by forming two H-bonds with the pyridine nitrogen (d_{H-N} = 2.122 Å) and Cbz amide proton (d_{O-H} = 2.397 Å), and two H-bonds (d_{O-H} = 2.371 and 2.382 Å) with the amide proton (Figure 3a) as well as other weak H-bonds of less than

dx.doi.org/10.1021/ja5077537 | J. Am. Chem. Soc. 2014, 136, 14270–14276

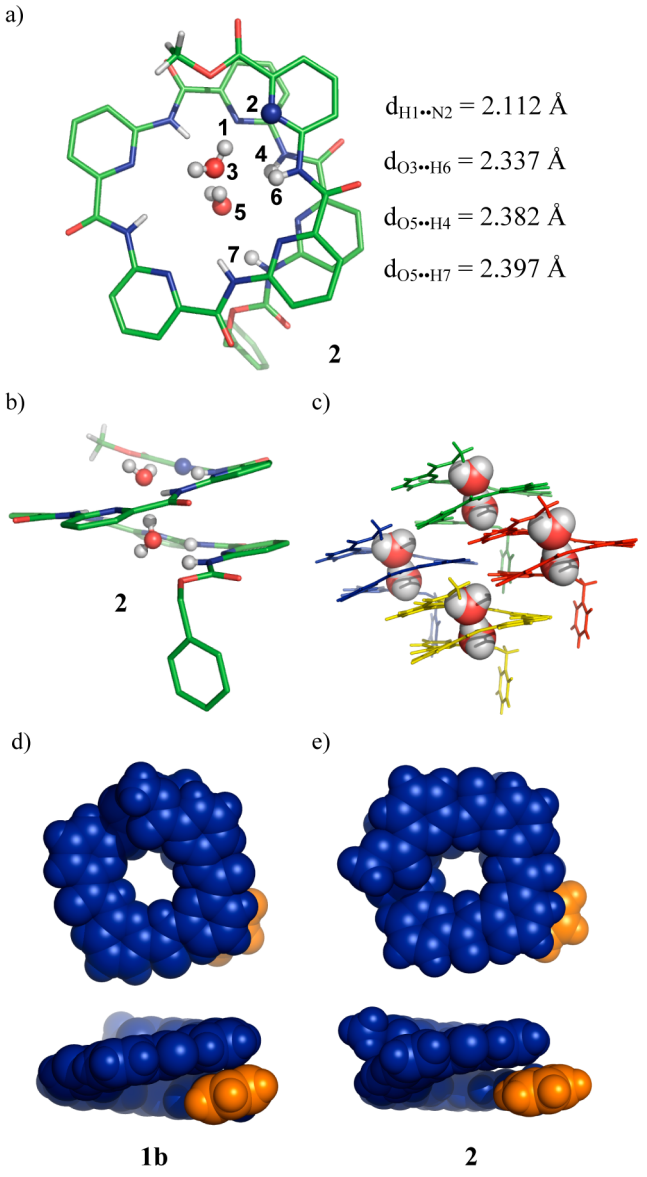

Figure 3. (a) Top and (b) side views of the crystal structure of hexamer **2** with its packing diagram in (c) that illustrates no defined 1D helical channel formed from **2**. (d) and (e) highlight a structural difference between pentamer **1b** being able to form 1D helical stacks via complementary "sticky" end groups and hexamer **2** that does not. Note that **1b** was taken from the crystal structure, and **2** was optimized at the B3LYP/6-31G(d) level on the basis of its crystal structure by forcing its twisted Cbz group shown in (b) to be aligned roughly parallel to the main helical backbone. The phenyl ring from the Cbz group in **1b** and **2** is in orange and the main backbone is in blue. These CPK illustrations show that the surface protrusion by the phenyl ring from the end Cbz group is more substantial in **2** than that in **1b**. This protrusion by the Cbz group in **2** subsequently disfavors the intercolumnar associations among 1D helical stacks, possibly accounting for the inability of **2** to produce organized 1D helical stacks.

3.0 Å between the host and guest molecules. The water dimer is additionally stabilized by forming two strong H-bonds of 2.027 and 2.105 Å with the carbonyl O atoms from the two neighboring hexamer molecules. Due to the twisted Cbz group that stays roughly perpendicular to the helical backbone (Figure 3b), molecules of **2** do not assemble to form the desired 1D helical stack. Instead, the hexameric backbones stack over each other via partial overlaps (Figure 3c). To understand if the twisted Cbz is the sole basis for the discrepancy between pentamer **1b** being able to form 1D stacks and hexamer **2** that does not, the Cbz group in **2** was allowed to have an orientation similar to that in **1b** and to stay roughly parallel to the main backbone, and geometric optimization was performed on this alternative structure at the level of B3LYP/6-31G(d).[7] Except for the Cbz group, the computationally optimized structure closely resembles the crystallographically determined helical structure of **2**. A comparative structural analysis between **1b** and optimized **2** now reveals a more significant surface protrusion by the Cbz group in **2**, which prevents efficient intercolumnar associations among 1D helical stacks (Figure 3d,e). This incompatibility between the Cbz group and the hexameric backbone in **2** possibly accounts for the inability of **2** to produce organized 1D helical stacks.

Going back to our original pentameric backbone, we thought that replacement of the pyridine with hydroxybenzene unit at the ester end as in **3a** and **3b** should not interfere with the end-to-end H-bond while providing H-bond donor and acceptor of different affinities for water binding (Figure 2a). Contrary to our intuition (Figure 4a,b), the end-to-end H-bond between

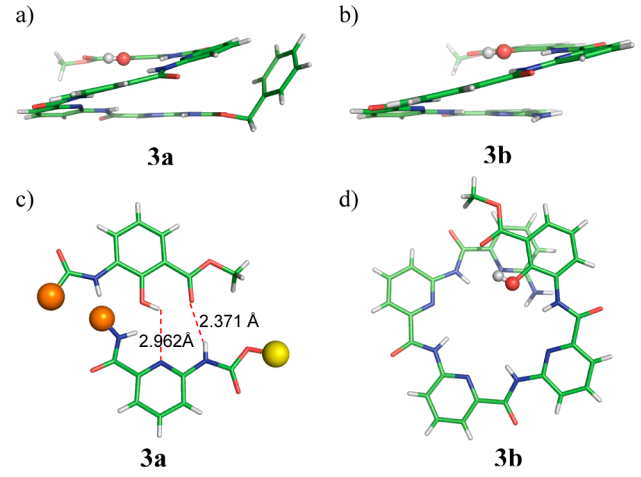

Figure 4. Helically folded structures of (a) **3a** and (b) **3b** in the solid state, (c) a tighter end-to-end association involving the ester end of one molecule of **3a** and the pyridine unit at the Cbz end of another molecule of **3a** via stronger intermolecular H-bonds; such intermolecular H-bonds may disrupt the weaker hypothetic H-bond pattern depicted in Figure 2b for **3a**, and (d) top view of the crystal structure **3b** with a shortened backbone, which is unable to maintain a full overlap of the helical backbones. In (c), the orange balls represent the remaining helical backbone, and yellow ball refers to the Cbz group.

the ester and twisted Cbz or amine groups as depicted in Figure 2b is not found in both **3a** and **3b** in the solid state, although they both still take up a helical geometry. For **3a**, this disruption results from a dimerization involving the ester end of one pentamer molecule and the pyridine unit at the Cbz end of another pentamer molecule via stronger intermolecular H-bonds of 2.371 and 2.962 Å (Figure 4c). The weakened end-to-end H-bonding interaction of 0.51 kcal/mol between the two "sticky" ends of **3a** (Figure 2b) with respect to 1.50 kcal/mol for **1b** (Figure 1d) further increases the chance of deviations from the "correct" structure intended for the desired 1D packing. As for **3b**, elimination of the end Cbz group produces a more rigid backbone, but shortens the helical backbone,

dx.doi.org/10.1021/ja5077537 | J. Am. Chem. Soc. 2014, 136, 14270−14276

resulting in possibly insufficient driving forces through aromatic $\pi-\pi$ contacts for stacking. Therefore, **3b** becomes unable to support energetically more favored full overlaps of the helical backbones (Figure 4d). Instead, partial overlaps are seen in its crystal structure.

Gratifyingly as illustrated in Figure 5, a replacement of the more flexible Cbz group with a rigid phenyl ring not only leads to the persistent formation of a helical structure in **4** but also renders molecules of **4** with an ability to form the desired 1D helical stacks mediated via H-bonding between the two "sticky" ends depicted in Figure 2b.[8] These 1D chiral stacks appear to be made up of a single polymeric chiral backbone rather than numerous short oligomers. Importantly, the 1D hollow cavity formed in $(\mathbf{4})_n$ is now able to accommodate H-bonded 1D water chains. All the 1D helical stacks in the crystal structure are exclusively made up of helices of the same handedness (Figure 5a), creating chiral aquapores with a narrow cavity of ~2.8 Å across.[9] The 1D water chains residing inside the chiral channels also adopt the same handed geometry with four water molecules per turn. These 1D chiral stacks further assemble into a 3D chiral crystal lattice via intercolumnar edge-to-edge contacts facilitated by the externally arrayed partially charged O and H atoms and by the discrete dichloromethane molecules occupying the intercolumnar spaces (Figure 5f).

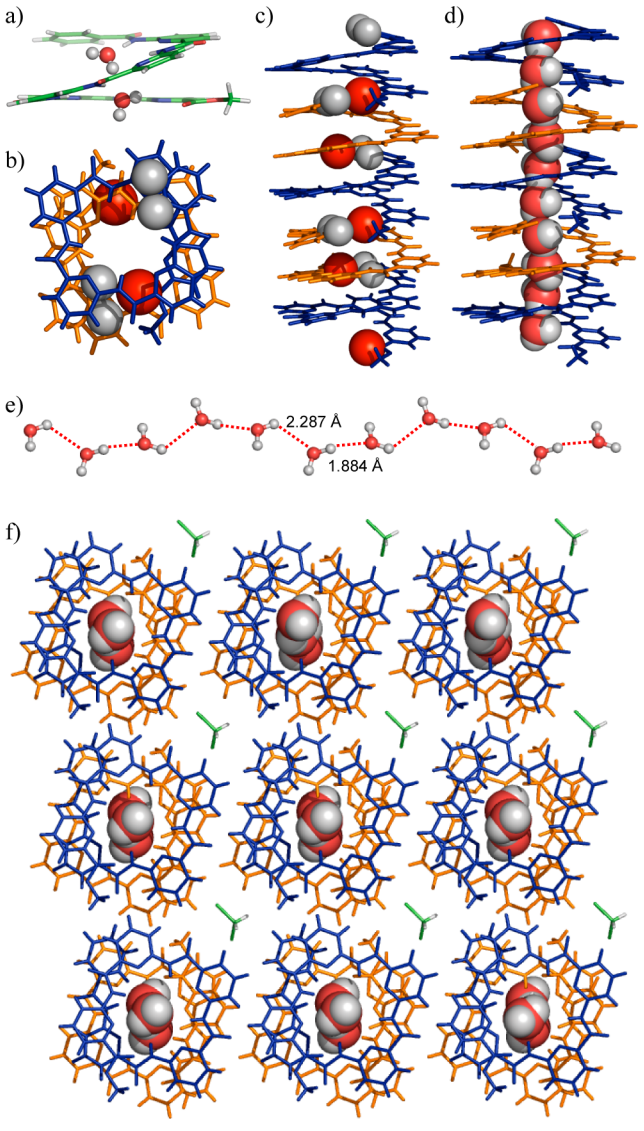

Figure 5. (a) Side view of the helical geometry taken up by **4** in the solid state, (b) top view of $(\mathbf{4})_n$ illustrating two sets of complementary end atoms each containing two H atoms in gray and one O atom in red that participate in forming two weak intermolecular H-bonds of C═O···H—C type (d_{O-H} = 2.746 and 2.821 Å, see Figure 2b). These H-bonds help create (c) 1D chiral helical stacks consisting of helices of the same handedness and (d) chiral aquapores of ~2.8 Å across for accommodating (e) H-bonded 1D water chains. (f) The two-dimensional array of nanotubes containing 1D water chains with discrete dichloromethane molecules occupying the intercolumnar spaces (projection down *b*-axis). In (b), an efficient full overlap involving the helical backbones is clearly visible.

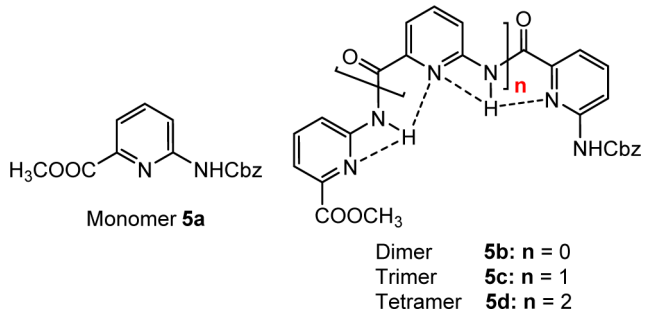

A quantitative understanding of the driving forces underlying the formation of 1D chiral stacks was obtained by carrying out computational investigations on aromatic $\pi-\pi$ stacking forces by using Dreiding force field,[10] and on water stabilization by the host and water chain by first principle calculation at the B3LYP/6-311G(2d,p) level. Energy calculations on the structural motifs taken out from the crystal structure yield the binding energies of varying components. Specifically, efficient aromatic stacking is the major driving force, contributing 29.75 kcal/mol per helical molecule of **4** to the formation of 1D chiral stack. This is cooperatively stabilized by weak yet indispensable intermolecular H-bonds of 2.26 kcal/mol arising from the "sticky" ends (Figure 2b). The host molecules of **4** provide average stabilization energy of 21.44 kcal/mol per water dimer largely via the formation of five H-bonds of 2.152, 2.374, 2.242, 2.517, and 2.168 Å in length between the water molecules and two amide H atoms, two pyridine N atoms and one ester O atom, respectively. Every water molecule in the water chain is further stabilized by the two adjacent water molecules through the formation of two strong intermolecular H-bonds of 1.884 and 2.287 Å with respective bond strengths of 4.15 and 3.60 kcal/mol (Figure 5e).

Following established protocols for investigating water transport with osmotic pressure induced by concentration gradient in salts such as NaCl,[5b,c] our repeated attempts to demonstrate the ability of **4** to transport water molecules across lipid membranes in large unilamellar vesicles (LUVs) with ~250 nm diameter proved unsuccessful. Nevertheless, both **4** and **1b** turn out to be good proton transporters (Figure 6). In a typical experimental setup, LUVs were first prepared from egg yolk L-α-phosphatidylcholine (EYPC) to entrap pH-sensitive dye 8-hydroxypyrene-1,3,6-trisulfonate (HPTS) at 0.1 mM in PBS buffer (NaCl = 100 mM, pH = 7.4). A 100 μL of such freshly prepared HPTS-trapped LUV suspension was then diluted into 2 mL of PBS buffer at pH = 5.5 to impose a pH gradient across the membranes of LUVs. This is followed by additions of 20 μL of 0.2 mM DMSO solution of **1a**, **1b**, **3a**, **3b**, **4**, **5a**-**5d** and gramicidin (1.45 mol % relative to lipid) or 20 μL

dx.doi.org/10.1021/ja5077537 | J. Am. Chem. Soc. 2014, 136, 14270−14276

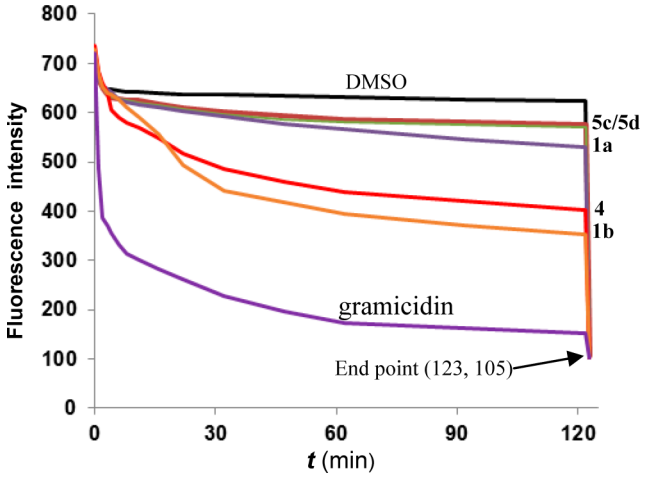

Figure 6. Time-dependent reductions in fluorescence intensity (λ_{ex} = 460 nm, λ_{em} = 510 nm) of HPTS inside the LUVs upon respective additions of 20 μL of 0.2 mM DMSO solution of **1a**, **1b**, **4**, **5c**, **5d** and gramicidin (1.45 mol % relative to lipid) or 20 μL of pure DMSO into 2 mL of PBS buffer containing 10 mM Na-phosphate and 100 mM NaCl. The pHs inside and outside the LUVs are 7.4 and 5.5, respectively. All the transport studied were carried out for 122 min, and stopped at t = 123 min by adding 50 μL of aqueous solution containing 5% triton x-100.

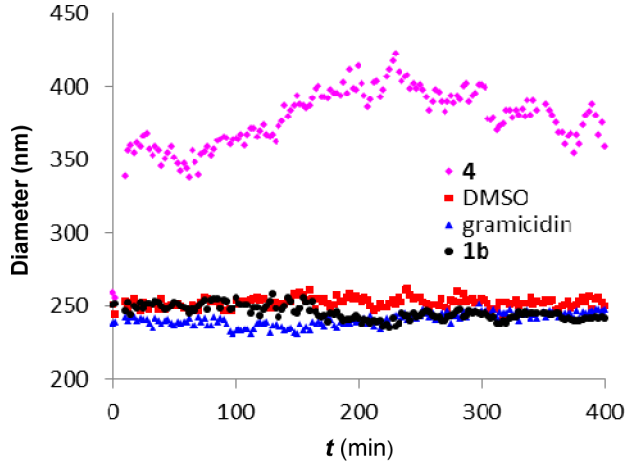

Figure 7. Dynamic light scattering experiments revealing time-dependent variations in diameters of LUVs upon respective additions of 10 μL of 0.2 mM DMSO solution of **1b**, **4** and gramicidin (1.45 mol % relative to lipid) or 10 μL of pure DMSO into 1 mL of PBS buffer containing 10 mM Na-phosphate and 100 mM NaCl. The pHs inside and outside the LUVs are 7.4 and 5.5, respectively. All the DLS experiments were monitored at 400 nm and carried out for 400 min.

of pure DMSO into the resultant LUV suspension. Since proton influx into LUVs invariably leads to reductions in the fluorescence intensity of HPTS trapped inside the LUVs, changes in fluorescence intensity of HPTS therefore can be correlated to the proton-transporting activities of the molecules. Figure 6 shows that **1b** and **4** have comparable activities, and transport protons to good extents in comparison with gramicidin A. On the other hand, oligomers such as monomer **5a** (Figure S1), dimer **5b** (Figure S1), trimer **5c** (Figure 6), tetramer **5d** (Figure 6), pentamers **3a** and **3b** (Figure S1) that are unable to form water-complexes as well as water-trapping aquapentamer **1a** (Figure 6) that is unable to stack all exhibit insignificant or weak proton-transporting activities. This strongly suggests a high likelihood for both **4** and **1b** to pile up to create a functional hollow cavity in the membrane that transports protons across the LUV membranes. Such a scenario is consistent with pore formation by **4** and **1b** in the solid states (Figures 1d and 2e,f). Given the fact that up to 40% of the methanol molecules residing inside the hollow cavity of $(\mathbf{1b})_n$ is able to exchange with water molecules upon contact with aqueous solution, it is possible that the observed proton transport for $(\mathbf{1b})_n$ is also mediated by the water molecules.

A very surprising finding was then obtained when the same LUV solutions for proton transport studies were subject to the examination by dynamic light scattering (DLS) analysis, a technique commonly used for determination of particle sizes. By monitoring light scattering at 400 nm, the average particle size of LUVs in the presence of **4** increases rapidly from ~250 to ~350 nm within the first 15 min, and to ~400 nm 3 h later. An average particle size of ~350 nm or above is well maintained within a period of 7 h. In contrast, molecules such as **1b** and gramicidin (Figure 7) as well as **1a**, **5c** and **5d** (Figure S2) that are unable to support the efficient formation of 1D water chains produce marginable changes in average particle size by 4.4, 4.1, 3.2, 4.4 and 7.0%, respectively.[11] For comparison, a corresponding change of 3.7% was observed from the control experiment using pure DMSO containing no compound (Figure 7). These comparative DLS results suggest that the water-transporting ability of **4** likely lead to initial swelling of the LUVs by ~10%,[11a] increasing the internal pressure that causes subsequent rapid vesicle fusions to produce larger LUVs of ≥350 nm.[11b] These data further point to the important and indispensable roles played by both the well-aligned 1D water chains inside $(\mathbf{4})_n$ and proton gradient, synergistically acting to create "osmotic pressure" for facilitating transport of water molecules across the membranes. The speculation on the "proton gradient-induced water transport" is quite intriguing in that no other synthetic systems on proton or water transports so far have demonstrated this unusual behavior.

Further considering that molecules of **4** enclose a narrow aquapore of ~2.8 Å in diameter, a size identical to the size of a water molecule, and that this small cavity further lacks the binding elements for liberating ions from their hydration shell, there is a high possibility for the 1D hollow aquapores formed by **4** to selectively pass water molecules or protons while excluding other ionic species. Our additional studies do reveal no detectable transport of alkali metal ions such as Na^+ and K^+ by **4**.

CONCLUSION

Our current investigation shows that the two "sticky" groups placed at the opposite ends of the helical molecules do not always equip the cavity-containing molecules with the ability to pack into well-defined 1D helical stacks containing 1D hollow cavities for hosting small guest molecules in a chain-like fashion. Presumably due to weak and fragile intermolecular H-bonds formed between "sticky" groups, factors such as surface overprotrusion by certain groups in the helical backbone as in hexamer **2**, the presence of stronger intermolecular H-bonds as in pentamer **3a**, or a shortened helical backbone as in pentamer **3b** all seem to be detrimental to the proper function intended to be performed by the end "sticky" groups. To promote the efficient formation of 1D helical stacks involving the short helices and to eventually produce the ordered 3D crystal lattice, the helical backbones need to be geometrically compatible with intermolecular forces of various types in a way

dx.doi.org/10.1021/ja5077537 | J. Am. Chem. Soc. 2014, 136, 14270−14276

to allow for (1) the attractive but weak end-to-end interactions via "sticky" ends to have a chance of synergistically working with stronger aromatic $\pi-\pi$ stacking forces to facilitate a full overlap of helical backbones and (2) the 1D columnar stacks to mutually stabilize each other by efficiently interacting with each other via intercolumnar edge-to-edge contacts.

In connection with their great diversities and demonstrated varying functions,[12] it is quite unusual to note that only one other type of water-binding foldamer molecules has been thus far elaborated, encapsulating up to three water molecules in their cavities.[13] Our foldamer-based approach presented here enables the unprecedented creation of hollow tubular aquapores in $(\mathbf{4})_n$ by one-dimensionally aligning short cavity-containing helices via the two complementary "sticky" groups located at the two helical ends. Crystallographically, the formed narrow chiral aquapores measuring ~2.8 Å in diameter are capable of hosting continuous H-bonded 1D water chains. Functionally, these well-aligned single-file water molecules demonstrate their ability to transport protons as well as water molecules in the presence of proton gradient across the lipid membranes. Fine-tuning the interior properties of aquapentamer **4** by replacing one or more pyridine units with other structurally similar and geometrically compatible methoxybenzene,[7a,b] pyridone,[14a,b] or fluorobenzene[14c,d] building blocks may produce channel molecules with differential transport activities across lipid membranes for interesting applications.

■ ASSOCIATED CONTENT

Supporting Information

Synthetic procedures for **2**–**4** as well as a full set of characterization data including ^{1}H NMR, ^{13}C NMR, (HR)MS, proton transport by **3a**, **3b**, **5a** and **5b**, DSL data for **1a**, **5c** and **5d** and computational details. This material is available free of charge via the Internet at http://pubs.acs.org.

■ AUTHOR INFORMATION

Corresponding Author

hqzeng@ibn.a-star.edu.sg

Present Address

[‖]Fujian Institute of Research on the Structure of Matter, Chinese Academy of Sciences, 155 West Yangqiao Road, Fuzhou 350002, China.

Author Contributions

[⊥]H.Z. and S.S. contributed equally to the work.

Notes

The authors declare no competing financial interest.

■ ACKNOWLEDGMENTS

This work was supported by the Institute of Bioengineering and Nanotechnology (Biomedical Research Council, Agency for Science, Technology and Research, Singapore), SPORE (COY-15-EWI-RCFSA/N197-1), and NRF CRP Grant (R-154-000-529-281).

■ REFERENCES

(1) Highly selective rapid water diffusion by aquaporins while blocking passage of even protons is assisted by (1) the narrowest pore diameter of ~ 3 Å, which is only slightly larger than the ~ 2.8 Å diameter of a water molecule and spans just one amino-acid residue, and (2) the two conserved asparagines in the center that lead to the opposite orientations of water molecules in the two halves of the channel that prevents the formation of a "proton" wire. See: (a) Murata, K.; Mitsuoka, K.; Hirai, T.; Walz, T.; Agre, P.; Heymann, J. B.; Engel, A.; Fujiyoshi, Y. *Nature* **2000**, *407*, 599. (b) Tajkhorshid, E.; Nollert, P.; Jensen, M. Ø.; Miercke, L. J. W.; O'Connell, J.; Stroud, R. M.; Schulten, K. *Science* **2002**, *296*, 525.

(2) (a) Hummer, G.; Rasaiah, J. C.; Noworyta, J. P. *Nature* **2001**, *414*, 188. (b) Wang, H. J.; Xi, X. K.; Kleinhammes, A.; Wu, Y. *Science* **2008**, *322*, 80. (c) Tei, Z. F.; Zhao, D. B.; Geldbach, T. J.; Scopelliti, R.; Dyson, P. J.; Antonijevic, S.; Bodenhausen, G. *Angew. Chem., Int. Ed.* **2005**, *44*, 5720.

(3) For 1D water chains hosted by organic hydrophilic pores, see: (a) Henrik, B.; Dieter, S.; Philip, P. *Angew. Chem., Int. Ed.* **2002**, *41*, 754. (b) Cheruzel, L. E.; Pometun, M. S.; Cecil, M. R.; Mashuta, M. S.; Wittebort, R. J.; Buchanan, R. M. *Angew. Chem., Int. Ed.* **2003**, *42*, 5452. (c) Sidhu, P. S.; Udachin, K. A.; Ripmeester, J. A. *Chem. Commun.* **2004**, 1358. (d) Saha, B. K.; Nangia, A. *Chem. Commun.* **2005**, 3024. (e) Ono, K.; Tsukamoto, K.; Hosokawa, R.; Kato, M.; Suganuma, M.; Tomura, M.; Sako, K.; Taga, K.; Saito, K. *Nano Lett.* **2009**, *9*, 122. (f) Duc, Y. L.; Michau, M.; Gilles, A.; Gence, V.; Legrand, Y.-M.; Lee, A.; Tingry, S.; Barboiu, M. *Angew. Chem., Int. Ed.* **2011**, *50*, 11366.

(4) For 1D water chains hosted by organic hydrophobic pores, see: (a) Raghavender, U. S.; Aravinda, S.; Shamala, N.; Kantharaju; Rai, R.; Balaram, P. *J. Am. Chem. Soc.* **2009**, *131*, 15130. (b) Raghavender, U. S.; Kantharaju; Aravinda, S.; Shamala, N.; Balaram, P. *J. Am. Chem. Soc.* **2010**, *132*, 1075. (c) Natarajan, R.; Charmant, J. P. H.; Orpen, A. G.; Davis, A. P. *Angew. Chem., Int. Ed.* **2010**, *49*, 5125.

(5) For water or proton transport mediated by pore-forming organic molecules, see: (a) Kaucher, M. S.; Peterca, M.; Dulcey, A. E.; Kim, A. J.; Vinogradov, S. A.; Hammer, D. A.; Heiney, P. A.; Percec, V. *J. Am. Chem. Soc.* **2007**, *129*, 11698. (b) Hu, C. B.; Chen, Z. X.; Tang, G. F.; Hou, J. L.; Li, Z. T. *J. Am. Chem. Soc.* **2012**, *134*, 8384. (c) Zhou, X. B.; Liu, G. D.; Yamato, K.; Shen, Y.; Cheng, R. X.; Wei, X. X.; Bai, W. L.; Gao, Y.; Li, H.; Liu, Y.; Liu, F. T.; Czajkowsky, D. M.; Wang, J. F.; Dabney, M. J.; Cai, Z. H.; Hu, J.; Bright, F. V.; He, L.; Zeng, X. C.; Shao, Z. F.; Gong, B. *Nat. Commun.* **2012**, 3. (d) Kim, A. J.; Kaucher, M. S.; Davis, K. P.; Peterca, M.; Imam, M. R.; Christian, N. A.; Levine, D. H.; Bates, F. S.; Percec, V.; Hammer, D. A. *Adv. Funct. Mater.* **2009**, *19*, 2930. (e) Si, W.; Chen, L.; Hu, X. B.; Tang, G. F.; Chen, Z. X.; Hou, J. L.; Li, Z. T. *Angew. Chem., Int. Ed.* **2011**, *50*, 12564.

(6) For our recent works on water-binding aquafoldamers, see: (a) Zhao, H. Q.; Ong, W. Q.; Fang, X.; Zhou, F.; Hii, M. N.; Li, S. F. Y.; Su, H. B.; Zeng, H. Q. *Org. Biomol. Chem.* **2012**, *10*, 1172. (b) Ong, W. Q.; Zhao, H. Q.; Du, Z. Y.; Yeh, J. Z. Y.; Ren, C. L.; Tan, L. Z. W.; Zhang, K.; Zeng, H. Q. *Chem. Commun.* **2011**, *47*, 6416. (c) Ong, W. Q.; Zhao, H. Q.; Fang, X.; Woen, S.; Zhou, F.; Yap, W. L.; Su, H. B.; Li, S. F. Y.; Zeng, H. Q. *Org. Lett.* **2011**, *13*, 3194.

(7) (a) Yan, Y.; Qin, B.; Shu, Y. Y.; Chen, X. Y.; Yip, Y. K.; Zhang, D. W.; Su, H. B.; Zeng, H. Q. *Org. Lett.* **2009**, *11*, 1201. (b) Yan, Y.; Qin, B.; Ren, C. L.; Chen, X. Y.; Yip, Y. K.; Ye, R. J.; Zhang, D. W.; Su, H. B.; Zeng, H. Q. *J. Am. Chem. Soc.* **2010**, *132*, 5869. (c) Zhao, H. Q.; Ong, W. Q.; Zhou, F.; Fang, X.; Chen, X. Y.; Li, S. F. Y.; Su, H. B.; Cho, N.-J.; Zeng, H. Q. *Chem. Sci.* **2012**, *3*, 2042. (d) Qin, B.; Chen, X. Y.; Fang, X.; Shu, Y. Y.; Yip, Y. K.; Yan, Y.; Pan, S. Y.; Ong, W. Q.; Ren, C. L.; Su, H. B.; Zeng, H. Q. *Org. Lett.* **2008**, *10*, 5127. (e) Qin, B.; Ren, C. L.; Ye, R. J.; Sun, C.; Chiad, K.; Chen, X. Y.; Li, Z.; Xue, F.; Su, H. B.; Chass, G. A.; Zeng, H. Q. *J. Am. Chem. Soc.* **2010**, *132*, 9564.

(8) The enhanced stability of structure **4** imparted by the terminal phenyl ring was similarly observed in Bell's helical system, see: Bell, T. W.; Jousselin, H. *Nature* **1994**, *367*, 441.

(9) Given a value of 0.26(12) for the absolute structure parameter for pentamer **4**, the absolute handedness of the helices in the chiral crystals of **4** cannot be confidently determined crystallographically. But to a good extent and counting from the ester to the phenyl ends, all the 1D helical stacks in the chiral crystals are likely made up of right-handed, rather than left-handed, helices with water chains adopting a right-handed geometry.

(10) (a) Mayo, S. L.; Olafson, B. D.; Goddard, W. A., III *J. Phys. Chem.* **1990**, *94*, 8897. (b) The first principles calculation at this level has consistently enabled us to accurately predict 3D topography of

oligomers of varying types that were later experimentally verified by the crystal structures. See ref 7.

(11) (a) It has been shown that simple vesicular swelling rarely exceeds by 10% of its original size. See: Haines, T. H.; Li, W.; Green, M.; Cummins, H. Z. *Biochemistry* **1987**, *26*, 5439. (b) Similar vesicle fusions to produce larger LUVs of ~ 370 nm from smaller ones of ~ 150 nm were previously observed. See ref 5b.

(12) For some selected reviews in foldamers, see: (a) Gellman, S. H. *Acc. Chem. Res.* **1998**, *31*, 173. (b) Hill, D. J.; Mio, M. J.; Prince, R. B.; Hughes, T. S.; Moore, J. S. *Chem. Rev.* **2001**, *101*, 3893. (c) Gong, B. *Acc. Chem. Res.* **2008**, *41*, 1376. (d) Saraogi, I.; Hamilton, A. D. *Chem. Soc. Rev.* **2009**, *38*, 1726. (e) Guichard, G.; Huc, I. *Chem. Commun.* **2011**, *47*, 5933. (f) Ong, W. Q.; Zeng, H. Q. *J. Inclusion Phenom. Macrocyclic Chem.* **2013**, *76*, 1. (g) Zhang, D.-W.; Zhao, X.; Hou, J.-L.; Li, Z.-T. *Chem. Rev.* **2012**, *112*, 5271. (h) Yamato, K.; Kline, M.; Gong, B. *Chem. Commun.* **2012**, *48*, 12142. Fu, H. L.; Liu, Y.; Zeng, H. Q. *Chem. Commun.* **2013**, *49*, 4127.

(13) For another class of water-binding foldamer molecules by Huc, see: (a) Garric, J.; Leger, J.-M.; Huc, I. *Angew. Chem., Int. Ed.* **2005**, *44*, 1954. (b) Garric, J.; Léger, J.-M.; Huc, I. *Chem.—Eur. J.* **2007**, *13*, 8454.

(14) (a) Ren, C. L.; Maurizot, V.; Zhao, H. Q.; Shen, J.; Zhou, F.; Ong, W. Q.; Du, Z. Y.; Zhang, K.; Su, H. B.; Zeng, H. Q. *J. Am. Chem. Soc.* **2011**, *133*, 13930. (b) Du, Z. Y.; Ren, C. L.; Ye, R. J.; Shen, J.; Lu, Y. J.; Wang, J.; Zeng, H. Q. *Chem. Commun.* **2011**, *47*, 12488. (c) Ren, C. L.; Xu, S. Y.; Xu, J.; Chen, H. Y.; Zeng, H. Q. *Org. Lett.* **2011**, *13*, 3840. (d) Ren, C. L.; Zhou, F.; Qin, B.; Ye, R. J.; Shen, S.; Su, H. B.; Zeng, H. Q. *Angew. Chem., Int. Ed.* **2011**, *50*, 10612.